

Determination of the Structural Role of the Linking Moieties in the DNA Binding of Adozelesin[†]

Linda Cameron and Andrew S. Thompson*

Department of Pharmacy and Pharmacology, University of Bath, Claverton Down, Bath, England. BA2 7AY

Received November 16, 1999

ABSTRACT: Adozelesin (formerly U73975, The Upjohn Co.) is a monofunctional DNA alkylating analogue of the antitumor antibiotic (+)-CC-1065. Adozelesin consists of a cyclopropa[*c*]pyrrolo[3,2-*e*]indol-4(5*H*)-one (CPI) alkylating subunit of (+)-CC-1065 and an indole and benzofurans subunit replacing the more complex pyrroloindole B and C subunits, respectively, of (+)-CC-1065. Previous studies have shown that adozelesin forms a reversible covalent DNA duplex adduct via a reaction between the N3 of adenine and the cyclopropyl of the cyclopropapyrroloindole (CPI) subunit. Gel electrophoresis studies have shown that adozelesin, like all the monofunctional (CPI)-based antitumor antibiotics, has a sequence preference for 5'-TTA*-3' [the asterisk (*) indicates covalently modified base]. Molecular-modeling studies have shown that the bound adozelesin ligand spans a total of five base pairs including the modified adenine. These studies have also indicated that, owing to the orientation of the ligand within the base minor groove, there should be an overall preference for sequences rich in A•T base pairs, thus avoiding steric crowding around the exocyclic NH₂ of any guanines present. In this study, we have prepared and studied, by high-field NMR and restrained molecular mechanics (rMM) and dynamics (rMD), the duplex adduct formed between adozelesin and 5'-CGTAAGCGCTTA*CG-3'. Previous molecular-modeling studies suggested that this sequence should be less preferred, since the two GC base pairs should lead to extensive steric crowding within the adduct, and this hypothesis has, however, never been supported by DNA-footprinting data. ¹H NMR of the adozelesin duplex adduct has revealed that, although Watson–Crick base pairing is maintained throughout the DNA duplex, there is significant distortion around the central base pairs. This distortion is the result of strong hydrogen-bonding between the amide linker of the indole and benzofuran subunits, and the carbonyl of a central thymine base and second, weaker, hydrogen bond to the exocyclic NH₂ of the central guanine was also observed. ¹H NMR and rMD also indicate that, to accommodate this hydrogen-bond system, the bound adozelesin is not positioned centrally within the minor groove but pushed toward the modified DNA strand. Previous studies on the dimeric CPI analogue bizelesin have indicated the important role the ureylene linker plays in the DNA binding. This study indicates that a similar situation exists in the reaction of adozelesin with double-stranded DNA and provides a possible explanation into the unpredicted sequence selectivity of these ligands.

The antitumor antibiotic (+)-CC-1065 was first isolated by scientists at The Upjohn Co. and is produced by *Streptomyces zelensis* (1, 2). On its discovery in 1974, (+)-CC-1065 was the most potent, low molecular weight compound known and showed cytotoxic potency and efficacy against a wide range of tumors in vitro (2, 3). Unfortunately, the subsequent discovery of an unusual delayed lethality in mice at subtherapeutic levels (4, 5) precluded (+)-CC-1065 from further clinical development. Following the initial success with (+)-CC-1065 in studies in vitro, The Upjohn Co. started a program to develop structurally related compounds. The aim of this study was to isolate the structural components of (+)-CC-1065 that were responsible for the cytotoxicity profile and the unusual delayed lethality. Adozelesin (6, 7), a monofunctional alkylator, and the DNA interstrand cross-linker bizelesin were the first of these “new

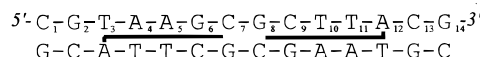
generation” CPI¹ synthetic analogues to be evaluated clinically, closely followed by the adozelesin related pro-drug carzelesin (U-80244).

Like the natural product (+)-CC-1065, adozelesin is overall right-handed, which mimics the pitch of B form DNA, allowing it to fit snugly within the minor groove of DNA. Previous studies have shown that adozelesin, like (+)-CC-1065, exerts its biological effect through alkylation of adenine N3 within the minor groove of DNA (Figure 1). Adozelesin also exhibits a high degree of molecular recognition for its binding site, the preferred consensus sequence being 5'-Pu,Py/Pu,TTA*[where the asterisk (*) depicts the site of alkylation] (8). High-field NMR studies on (+)-CC-1065 and on bizelesin have shown that the active functional-

[†] This research was funded by grants from the University of Bath and Association for International Cancer Research (AICR). Adozelesin was a gift from The Upjohn Co.

* To whom correspondence should be addressed.

¹ Abbreviations: CPI, cyclopropapyrroloindole; BP, base pair; NMR, nuclear magnetic resonance; NOE, nuclear Overhauser effect; NOESY, two-dimensional NOE correlated spectroscopy; rMD, restrained molecular dynamics; rMM, restrained molecular mechanics; FID, free induction decay; DMF, dimethylformamide; EDTA, ethylenediamine-tetraacetic acid; HPLC, high-performance liquid chromatography.



Previous molecular modeling (9) and NMR studies (13) on (+)-CC-1065 have indicated that the anionic phosphate oxygen of a base pair that two base pairs to the 5'-side of the modified adenine (on the noncovalently modified strand) may also be involved in hydrogen bonding with the phenolic proton of the CPI subunit. This hydrogen bonding has been used to explain the unusual downfield shift observed in several bizelesin (13, 14, 15) and (+)-CC-1065 (12) duplex adducts. However, no evidence for a hydrogen bond was found within the duplex adduct formed in the reaction of bizelesin with 5'-TAAAAA-3' (16). Studies using ^{17}O -labeled phosphates confirmed the presence of a hydrogen bond in the (+)-CC-1065 duplex adduct. However, it was observed between the phenolic proton on the CPI subunit and the

NMR studies on the DNA-DNA cross-linker bizelesin with 5'-TAATTA-3' have indicated the presence of two adduct conformations, both containing unusual base-pair conformations within the central A·T base pairs (13, 14). In the first case (60% of the observed species), the central base pairs were found to be Hoogsteen base paired. In contrast, in the second conformation, the bases were found to be in non-hydrogen-bonded open conformation. The unusual base-pair conformations observed within this sequence are believed to be the result of inherent instability within the 5'-TAATTA-3' sequence and the ability of bizelesin to stabilize these transient conformations via the ureylene linker prior to cross-link formation. Studies on an unusual seven base-pair cross-linked adduct formed between bizelesin and 5'-TTAGTTA-3' again outlined the important role the ureylene linker can play in the sequence specificity of these CPI ligands (16). Within this sequence, a strong hydrogen bond is formed between the exocyclic NH₂ of the central guanine and the carbonyl of the ureylene linker, while weaker hydrogen bonds form between the amido protons and the oxygen of a deoxyribose sugar. Interestingly, no unusual hydrogen bonding is observed from the ureylene linker within the adduct formed between bizelesin and the A-tract containing sequence 5'-TAAAAA-3' (18).

EXPERIMENTAL PROCEDURES

Chemicals. Adozelesin was a gift from The Upjohn Co. and was used without additional purification. Reagents used to prepare the NMR buffers, sodium hydrogen phosphate (99.99%), sodium chloride (99.99%), and EDTA (99.99%), were purchased from Fisons. HPLC grade acetonitrile, acetic acid, and methanol were purchased from Fisons. Reagents and solvents for automated DNA synthesis were purchased from Cruachem. DNA-grade Bio-Gel hydroxyapatite was purchased from Bio-Rad.

Oligonucleotide Preparation and Purification for NMR Studies. The single strand (5'-CGTAAGCGCTTA*CG-3') was synthesized on $2 \times 15\text{-}\mu\text{mol}$ scale using automated solid-phase phosphotriester and phosphoramidite chemistry (19) on an Applied Biosystems automated DNA synthesizer (model 381A), leaving the trityl protecting group on each of the strands. Each strand was deprotected overnight in saturated aqueous ammonia, followed by purification by reversed-phase HPLC, as outlined previously (18) DNA was detritylated using 50% aqueous acetic acid and reduced to dryness, followed by further purification by HPLC. The sample was desalted (dialysis) and then annealed in NMR buffer (10 mM NaH_2PO_4 /100 mM NaCl/0.1 mM EDTA, pH 6.85). The annealed sample was purified on a hydroxyapatite column using a gradient mobile phase (10–150 mM NaH_2PO_4 buffer, pH 6.85), before being desalted on a G-25 column and lyophilized to dryness. The purified DNA sample was redissolved in 500 μL of NMR deuterated buffer and a ^1H NMR sample was recorded; only duplex signals were observed.

Adduct Preparation and Purification for NMR Studies. The adozelesin adduct was prepared by stirring adozelesin (5 mg)

in deuterated DMF (0.2 mL) with 30 μ mol of the purified 14-mer in 600 μ L of twice-concentrated deuterated NMR buffer (pH 6.85). The reaction was followed by ^1H NMR, and after 24 h at 5 $^\circ\text{C}$, a mixture of duplex and duplex-adduct signals was observed. The sample was lyophilized to remove the solvent, resuspended in D_2O (600 μ L), and a second portion of adozelesin (5 mg) was dissolved in 0.2 mL of deuterated DMF added. The mixture was again allowed to stir at 5 $^\circ\text{C}$ for 24 h, and a ^1H NMR spectrum was recorded. One-dimensional ^1H NMR this time revealed only duplex adduct signals. The sample was again lyophilized to dryness and desalted. Excess drug was then removed on C_{18} Sep-Pak cartridges, and the sample was lyophilized to dryness and then redissolved in deuterated NMR buffer.

Proton NMR Experiments. One- and two-dimensional 400 and 600 MHz NMR data sets were recorded in H_2O and D_2O buffered solutions on JEOL EX400 (400 MHz) and Varian Innova 600 (600 MHz) spectrometers. Proton signals were recorded in parts per million (ppm) and referenced relative to the residual water signal (4.71 ppm).

Phase-sensitive two-dimensional NOESY spectra (JEOL and Varian) were obtained for mixing times 200, 250, and 300 ms (JEOL) and 250 ms (Varian). JEOL 400 MHz spectra were recorded with 64 scans at each of 1024 t_1 values at a spectral width of 10.002 ppm at a relaxation delay of 10 s between scans. The Varian 600 MHz NOESY data were acquired at 250 ms with 32 scans at each of 1024 t_1 values at a spectral width of 10.002 ppm at a relaxation delay of 2 s between scans. Two-dimensional NOE spectra in 90% H_2O at 150 ms mixing time were recorded using a 1-1 echo read pulse sequence (20, 21) with a 2 s pulse repetition delay and a sweep width of 25.025 ppm. Spectra were processed in the TRIAD module of the SYBYL software suite. During data processing, a 90 $^\circ$ -shifted sine-bell function was used in both ω_1 and ω_2 dimensions. The FID in ω_1 was zero-filled to 2K, prior to FT to give a 2K x 2K spectrum. DQF-COSY, TOCSY, and ROESY spectra were also recorded on the JEOL 400 MHz and Varian 600 MHz spectrometer and were used to confirm assignments made in the NOESY spectra. In addition, selected ^{13}C resonances were identified using a heteronuclear multiple-quantum coherence experiment in D_2O (22).

Molecular Modeling. Due to the self-complementary nature of this sequence the top seven base pairs of the self-complementary duplex were modeled. An additional pair of base pairs (G•C) was added to the top and bottom of the duplex to give an 11-mer; this approach significantly reduced the possibility of terminal base pairs fraying within the calculations, but leaving the central 7-mer free from artificial restraints. The DNA duplex was built using the Bio Polymer module of SYBYL and the adozelesin ligand was docked in the minor groove. Charges were then calculated for the complete complex using the Gasteiger-Hückel set of charges (23, 24). Counterions were placed on the O–P–O bisector at a distance of 6 Å from the phosphorus atom prior to solvation (25). The system was solvated as a droplet using six layers of solvent via the Molecular Silverware algorithm (26).

Restrained Molecular Dynamics Simulations. Interproton distance constraints were generated from the NOESY data in TRIAD and were incorporated into the adduct model using a weak (4–7 Å), medium (3–5 Å), and strong (1–3.5 Å)

methodology (27). The rMD calculations were performed using the Tripos Associates force fields within the SYBYL software suite on a SGI R4000 and SGI R3000 Indy workstations. The molecular dynamics calculations (in aquo) were performed at constant volume, using 2 fs time steps. The equilibrium protocol consisted of 100 steps of steepest descents minimization, follow by conjugate gradient minimization, applied to the solvent molecules to relax possible steric clashes at the adduct/solvent interface (28). The water was then thermalized at 300 K for 5 ps using a Boltzman initial velocity distribution, constant dielectric function, and fixed DNA with counterions. Finally, the molecular dynamics was performed with only the DNA fixed with the counterions and water mobilized at 300K for 5 ps. The rMD calculations on the complete solvated complex were started at 0 K and ramped over 50 ps in 10 steps to 300 K. Alternative starting structures were (1) Adozelesin 7-mer nonrestrained molecular dynamics products and (2) minimized B-DNA adducts. During the first 50 ps, the 376 NMR-derived distance restraints (68 of which were related to the bound adozelesin, Table 2) were applied to the system along with addition distance restraints, which were applied between the base pairs and to the counterions. During the next 6 ps, the non-NMR-derived distance restraints were removed from all but the two 5' and 3' terminal bases (G•C), which were left in place to prevent the duplex from fraying at elevated temperatures. The in vacuo and solvated systems were then held at 300 K for 60 ps, and the data for the last 50 ps (501 structures) was used to study hydrogen-bonding information. These data were then averaged and minimized to generate the averaged in vacuo and solvated structures (see later).

RESULTS

Assignments of the Proton Resonances for the Adozelesin 14-mer Duplex adduct. (1) Duplex Base and Deoxyribose Nonexchangeable Proton Assignments. The nonexchangeable protons of the self-complementary duplex (5'-CGTAAGCGCTTACG-3') and duplex adduct (5'-CGTAAGCGCTTA*CG-3') were assigned as outlined in previous (+)-CC-1065 and bizelesin studies (3, 13, 15, 18). A single set of 14 aromatic H6/H8 to H1', H2', and H2'' were observed as would be expected for a palindromic DNA duplex, confirming that a single adduct incorporating two identical adozelesin binding sites had formed (Figures 2a and 3b). Previous studies with the related dimeric CPI analogue, bizelesin, indicated the presence of unusual open and Hoogsteen base-pair configurations within the duplex adduct. To avoid missing any structures within this duplex adduct, the identities of the adenine H8 and H2 protons were confirmed by measuring the ^{13}C shift of the carbons connected to the aromatic protons (unpublished data). The values obtained for adenines A4, A5, and A12 confirm the absence of Hoogsteen or open base pairing (previously observed within the bizelesin adduct formed with 5'-TAATTA-3') (13). A summary of the nonexchangeable DNA proton assignments for the DNA duplex and the DNA duplex adduct is given in Table 1A.

(2) Adozelesin Nonexchangeable Proton Assignments. Adozelesin was divided into its three constituent subunits; cyclopropapyrroloindole (CPI) head unit (A), an indole (B), and a benzofuran unit (C) to facilitate assignment of the nonexchangeable protons (29). The aromatic protons in the benzofuran subunit (C) can be easily identified within the

Table 1: Chemical Shifts for All the Protons in the Adozelesin d(CGTAAGCGCTTACG) Duplex Adduct

(A) Chemical Shifts (ppm) of Nonexchangeable Protons in the d(CGTAAGCGCTTACG) Duplex Adduct at Room Temperature ^a										
	H8/H6	H2/H5/CH3	H1'	H2'	H2'2	H3'	H4'	H5'1	H5'2	imino
C1	7.51 <i>-0.03</i>	5.74 <i>-0.04</i>	5.58 <i>-0.08</i>	1.80 <i>-0.13</i>	2.20 <i>-0.13</i>	4.57 <i>-0.04</i>	3.93 <i>-0.05</i>	3.92 <i>0.34</i>	3.55 <i>-0.08</i>	
G2	7.83 <i>-0.06</i>		5.72 <i>-0.16</i>	2.46 <i>-0.13</i>	2.51 <i>-0.18</i>	4.83 <i>-0.06</i>	3.97 <i>-0.29</i>	3.95 <i>-0.07</i>	3.79 <i>-0.15</i>	13.41
T3	7.33 <i>0.19</i>	1.56 <i>0.14</i>	5.14 <i>-0.35</i>	2.19 <i>0.26</i>	2.37 <i>0.11</i>	4.80 <i>0.03</i>	4.15 <i>0.09</i>	4.02 <i>-0.01</i>	3.98 <i>-0.05</i>	11.45
A4	8.22 <i>0.08</i>	7.81 <i>0.41</i>	6.07 <i>0.30</i>	2.57 <i>-0.05</i>	2.77 <i>-0.02</i>	4.91 <i>-0.05</i>	4.28 <i>-0.02</i>	4.10 <i>-0.02</i>	4.06 <i>0.13</i>	
A5	7.65 <i>-0.30</i>	7.86 <i>-0.97</i>	5.70 <i>-0.14</i>	2.10 <i>-0.40</i>	2.48 <i>0.13</i>	4.45 <i>-0.49</i>	4.30 <i>-0.02</i>	3.66 <i>-0.47</i>	3.02 <i>-1.09</i>	
G6	6.82 <i>-0.56</i>		4.64 <i>-0.92</i>	1.60 <i>-0.72</i>	1.68 <i>-0.80</i>	4.27 <i>-0.55</i>	4.01 <i>-0.07</i>	3.79 <i>-0.46</i>	3.61 <i>-0.51</i>	12.61
C7	6.74 <i>-0.35</i>	4.61 <i>-0.42</i>	5.11 <i>-0.43</i>	1.20 <i>-0.59</i>	1.72 <i>-0.53</i>	4.50 <i>-0.39</i>	4.10 <i>0.07</i>	3.80 <i>-0.46</i>	3.45 <i>-0.56</i>	
G8	7.58 <i>-0.17</i>		5.83 <i>0.04</i>	2.41 <i>-0.45</i>	2.65 <i>0.04</i>	4.79 <i>-0.08</i>	4.08 <i>-0.19</i>	3.80 <i>-0.15</i>	3.45 <i>-0.42</i>	12.55
C9	7.19 <i>-0.10</i>	5.22 <i>0.02</i>	5.82 <i>-0.01</i>	1.83 <i>-0.17</i>	2.18 <i>-0.25</i>	4.34 <i>-0.32</i>	4.14 <i>0.01</i>	4.03 <i>-0.15</i>	3.81 <i>-0.28</i>	
T10	7.16 <i>-0.19</i>	1.37 <i>-0.14</i>	5.75 <i>-0.16</i>	1.73 <i>-0.30</i>	2.27 <i>-0.19</i>	4.34 <i>-0.43</i>	2.08 <i>-2.00</i>	3.30 <i>-0.73</i>	2.79 <i>-1.19</i>	14.41
T11	7.06 <i>-0.25</i>	1.45 <i>-0.18</i>	5.10 <i>-0.51</i>	1.53 <i>-0.51</i>	1.62 <i>-0.73</i>	4.39 <i>-0.41</i>	2.58 <i>-1.46</i>	3.71 <i>-0.31</i>	3.56 <i>-0.44</i>	14.02
A12	8.38 <i>-0.45</i>	7.96 <i>0.64</i>	5.75 <i>-0.33</i>	2.54 <i>-0.08</i>	2.81 <i>0.05</i>	4.83 <i>-0.11</i>	4.27 <i>-0.09</i>	4.18 <i>0.08</i>	3.79 <i>-0.25</i>	
C13	7.21 <i>-0.03</i>	5.54 <i>0.28</i>	5.24 <i>-0.30</i>	1.58 <i>-0.18</i>	2.02 <i>-0.17</i>	4.49 <i>-0.18</i>	4.02 <i>-0.04</i>	3.67 <i>-0.49</i>	3.35 <i>-0.66</i>	
G14	7.80 <i>-0.01</i>		5.99 <i>-0.03</i>	2.23 <i>-0.03</i>	2.53 <i>0.04</i>	4.60 <i>0.04</i>	4.15 <i>0.18</i>	4.03 <i>-0.05</i>	3.76 <i>-0.20</i>	12.32
(B) Proton Chemical Shifts (ppm) for the Bound Adozelesin at Room Temperature ^a										
CPI subunit										
H3	NH5	H6	CH3	H8A2	H8A	H8B	H1A	H1B		
7.985		6.98	2.546	4.495	5.063	5.155	3.689	3.812		
indole subunit										
benzofuran subunit										
NH1'1	H3'1	H4'1	H6'1	H7'1	NH9'1	H3'2	H4'2	H5'2	H6'2	H7'2
	7.283	7.805	8.243	7.629		7.651	7.932	7.497	7.373	7.736

^a Chemical shift differences $\delta_{\text{DNA-drug}} - \delta_{\text{DNA}}$, are shown in italics; shift differences greater than 0.25 ppm are underlined. Sample was dissolved in 0.5 mL of D₂O buffer containing 0.1 M sodium chloride and 10 mM sodium dihydrogen phosphate, pH 6.85, at 300 K.

COSY and TOCSY data due to the large ortho couplings. Hence, it is possible to easily identify protons H4'', H5'', H6'', and H7''. The last aromatic proton H3'' can be easily identified by an intense NOE to H4''. The H6' and H7' aromatic protons in the indole subunit (B) are ortho coupled and, hence, can be easily identified in the COSY and TOCSY data. However, H3' and H4' could only be assigned using the NOE data. Assignments for the CPI subunit were based on a combination of NOE and COSY data. Aromatic H6 and the CPI methyl were assigned from the COSY spectra. Assignments for the methylene protons H8A, H8B, H1A, and H1B, which have very similar chemical shifts, were assigned using NOE data from the CPI methyl, adenine (A12) H2, and the indole subunits H3'. To distinguish signals H8A from H8B, relative NOE intensities from H8A2 were measured. Similarly, H1A and H1B were identified from relative NOE intensities from H8A2 and the H3' from the indole subunit. The last unidentified aromatic signal was assigned as H3 based on NOE cross-connectivities to adenine (A12) H2. The complete assignment for the adozelesin is given in Table 1B.

(3) *DNA and Adozelesin Exchangeable Proton Assignments.* Two-dimensional NOE (H₂O) experiments were

conducted, and the exchangeable signals were assigned based on their connectivity networks into the aromatic region and imino protons of neighboring bases. All exchangeable signals were identified within the duplex adduct, except for those associated with the terminal bases. The imino signal of the thymine paired to the covalently modified adenine (A12) was significantly upfield-shifted as previously reported in (+)-CC1065 (10) and bizelesin (13, 15, 16), partially confirming the site of covalent attachment. The CPI subunit (A) and indole subunit (B) NH amine protons were identified by connectivities into the neighboring aromatic protons. The CPI phenol proton was identified on the basis of connectivity into the neighboring aromatic H3. The chemical shift of the phenolic proton at 13.52 ppm is consistent with 13.62 ppm observed within the previously reported (+)-CC-1065 adduct (10) and 13.05 and 13.80 within the A-tract bizelesin adduct (15). However, it contrasts with 11.06 and 11.10 ppm observed within the bizelesin 7-base-pair cross-linked adduct (16). Studies using ¹H NMR coupled with ¹⁷O-labeled water and phosphates in the (+)-CC1065 adduct confirmed that the phenolic proton in the (+)-CC1065 adduct was hydrogen-bonded (via an ordered water molecule) to the phosphate backbone (3). On the basis of the similarity of chemical shifts

Table 2: Intensities^a of the NOE Connectivities between Adozelesin and the Covalently Modified Duplex

	CPI subunit								indole subunit				benzofuran subunit				
	H3	H6	CH3	H8A2	H8A	H8B	H1A	H1B	H3'1	H4'1	H6'1	H7'1	H3'2	H4'2	H5'2	H6'2	H7'2
T3H1'			M														
A4H1'	W								W								
A4H2				W			W	M	W								
A5H2				M			W	W	W								
A12H1'	M		W														
A12H2		M	W		M	M	W	M									
C13H1'			W														
T11H1'									M								
T11H3'									M								
T11H4'									W	W	M	M					
A5H5'1									M								
A5H5'2									M								
A4H4'									M								
G6H2'1										W			W				
C7H4'											W						
C7H5'1											M		W				
C7H5'2											M						
T11H5'1											M						
T11H5'2											M						
A12H5'1												W					
G6H2'2													M				
T10H2'2													W				
C7H1'														M			
G8H1'														M	M	W	
C9H1'														M	M	W	
C9H2'1														M			
C9H2'2														W			
C9H3'														W			
C9H4'														M	M		
C9H5'2															W		
T10H1'														W			
T10H4'														M	M	M	M
T10H5'1														M	M	M	M
T10H5'2														W	M	M	M

^a W = weak, M = medium, and S = strong (relative to cytosine H5 to H6 cross-peak intensities).

observed, it would appear that a similar hydrogen bond is formed within this adduct. Signals for the amide NH proton between the indole (B) and benzofuran unit (C) could not be identified in either one- or two-dimensional ¹H NMR data. A summary of the exchangeable DNA proton assignments for the DNA duplex adduct are given in Table 1.

Two Adozelesin Molecules Are Bound within the Minor Groove Covalently Attached through N3 of Adenine (A12). Within the duplex adduct, there is a single aromatic to H1' and H2',H2'' walk, confirming that there are two adozelesin molecules bound within the minor groove, resulting in a symmetrical adduct. There are also sufficient DNA–adozelesin connectivities (68 in total) to confirm the location of the three adozelesin subunits within the minor groove. Connectivities from the adenine H2 proton of the modified adenine (A12) confirm the site of covalent modification (Figure 3). There are strong connectivities from the H2 proton of modified adenine (A12) into the protons of the bridging methylene (H8A and H8B) and the CPI subunits H1A, H1B, H8A2, and methyl. There are also weaker connectivities into the indole subunits H3' and H4'. Connectivities from the other adenine H2 protons (A4 and A5) into the indole and benzofuran subunit aromatic protons (H3', H4', and H3'') confirm the location and orientation of the adozelesin within the minor groove (Figure 2). No cross-peaks are observed from protons in the base of the minor groove to the adozelesin aromatic protons H3, H6', H7', H6'', and H7''. However, cross-peaks are evident to these aromatic

protons from H4' protons located high on the wall of the modified strand, confirming that the adozelesin is bound in an edge on in the minor groove. A complete list of adozelesin–duplex connectivities is provided in Table 2.

Benzofuran Subunit of the Adozelesin Molecule Associates More Closely with the Modified DNA Strand. NOE connectivities are observed from protons on the CPI and indole subunits into both the modified and nonmodified DNA strands. NOE connectivities are present both for protons in the base of the minor groove and from ribose protons (H4') high on the walls of the minor groove into aromatic protons on the back face of the CPI (H6) and indole (H6'1 and H7'1) subunits. From the ¹H NMR NOESY data, there are several NOE connectivities from the aromatic protons on the benzofuran subunit (H3'2, H4'2, and H5'2) into protons into the base of the minor groove. There are also connectivities from protons on the back face of the benzofuran (H6'2 and H7'2) into protons high on the walls of the minor groove (H4'), confirming its orientation within the groove. However, all of the observed connectivities are between the aromatic protons of the benzofuran and the modified DNA strand. This indicates that the benzofuran ring system is more closely associated with the covalently modified strand and is not situated centrally within the base of the minor groove, as would be predicted and was previously observed with CPI duplex adducts.

NMR Data Indicate That Normal Watson–Crick Base Pairing Is Maintained throughout the Duplex Adduct.

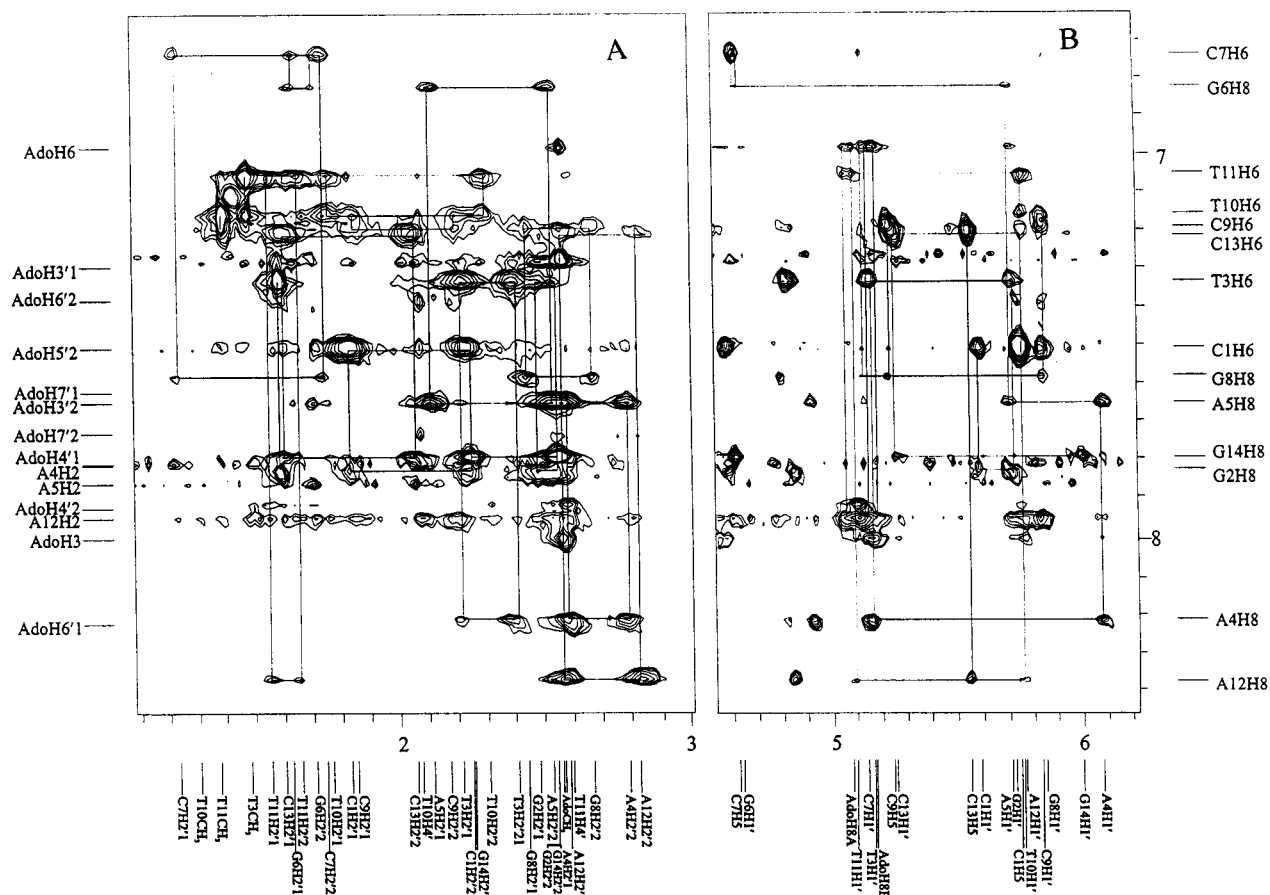


FIGURE 2: Two-dimensional phase sensitive NOESY spectrum (250 ms mixing time) expanded contour plot of the adozelesin duplex adduct in buffered D_2O solution, pH 6.75, at 300 K, displaying (a) connectivities for aromatic PuH8/PyH6 to deoxyribose H1' and deoxyribose H1' of the 5'-neighbor and (b) connectivities for aromatic PuH8/PyH6 to deoxyribose H2' and 2'' of the 5'-neighbor.

However, It Also Indicates Unusual Distortion around the Central Guanine (G6). 1H NMR data (confirmed with ^{13}C NMR data, unpublished data) show the presence of a single Watson–Crick base-paired duplex adduct. There is, however, evidence for significant distortion around guanine (G6) with enhanced connectivities into the 5'-neighboring base and sugar and weaker connectivities into the 3'-neighboring base and sugar. This would appear to be similar to distortion reported in a previously studied (+)-CC-1065 (3, 17), where a cytosine 3 base pairs away from the site of covalent modification adopted a C3'-endo conformation.

Restrained Molecular Dynamics Studies on the Adozelesin Duplex Adduct Show the Nature of Distortion around G6 and Provides an Insight into the Role of Linking Moieties in the Sequence Specificity of Adozelesin toward This Sequence. The molecular dynamics studies provide an averaged structure (Figure 5) that can be used to explain some of the unusual features within the 1H NMR data, indicating distortion in the center of the duplex adduct. The distortion is focused around thymine (T10) and guanine (G6) where the guanine is distorted into the minor groove and toward the center on the duplex, although Watson–Crick base pairing is maintained. Examining the distances between the hydrogen-bond donor and acceptor functionalities of thymine (T10) and guanine (G6) to the amide-linking moiety between the indole and benzofuran, hydrogen-bonding opportunities can be envisaged (Figure 4). A strong interaction is observed between the carbonyl on thymine (T10) and the NH of the amide linker (average distance 2.11 Å) and a

second weaker interaction between the exocyclic NH_2 of guanine (G6) and the carbonyl of the amide linker. To accommodate this second interaction, repositioning of the guanine base into the minor groove of the helix leads to distortion of its associated sugar, and this sugar now adopts a distorted C3'-endo geometry. This model is supported in the unusual intensities observed in the NOESY and couplings in the COSY data (30). Throughout the last 60 ps of the rMD calculations, these hydrogen bonds are fully occupied. Furthermore, it is the presence of this hydrogen bonding and distortion of the associated guanine (G6) that “pushes” the benzofuran out of the center of the minor groove toward the covalently modified strand.

DISCUSSION

One- and two-dimensional 1H and ^{13}C NMR analysis of the adozelesin duplex adduct reveal the presence of a single palindromic DNA duplex, containing two identical adozelesin-binding sites. The covalently bound adozelesin residues are bound to adenines (A12) in the minor groove, and normal Watson–Crick base pairing is maintained throughout the duplex adduct. NOE connectivities between the bound adozelesin molecules and the DNA duplex determine the location of drug within the minor groove but also show that the adozelesin is bound edge on into the minor groove. Connectivities from the methyl protons of the CPI subunit and the H2 proton of the modified adenines confirm that adenine A12 is the covalently modified base and that N3 is the site of covalent modification. The chemical shift of the

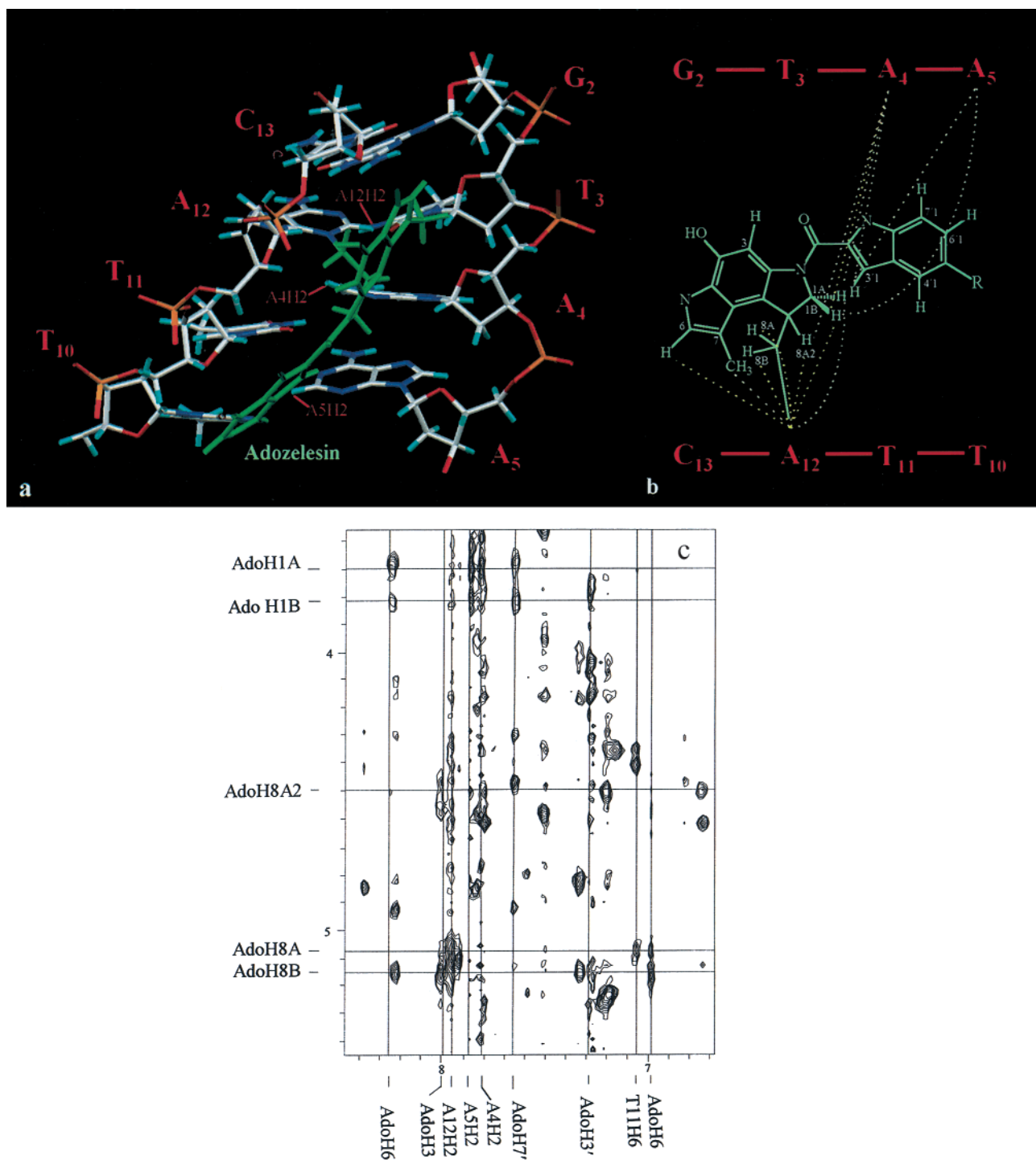


FIGURE 3: NOE connectivities between select adenine H2 protons and the bond adozelesin geminal H8A2, H1A, H1B, H8A and H8B protons. (a) Relative positions of the adenine H2 protons. (b) Relative intensities of the adenine H2 connectivities. (Intense peaks are shown in dashed yellow, intermediate peaks in dashed white). (c) Contour plot of the NOESY data showing the adenine H2 to ligand H8A2, H1A, H1B, H8A, and H8B protons.

CPI subunits phenol indicates that, as previously observed with (+)-CC-1065 (3) and bizelesin adducts (13, 15), a hydrogen bonding exists between these phenolic protons and the phosphate backbone. From the NOE contacts between the adozelesin and the DNA duplex, it is clear that the adozelesin indole and benzofuran subunits are associated more closely with the modified rather than with the unmodified DNA strand. This compares with the (+)-CC1065 duplex adduct (17), in which the B subunit was found to be more closely associated with the nonmodified DNA strand

and the C subunit with the covalently modified strand. This would appear to indicate that either the target sequence or subtle differences in ligand structure has a direct effect on the relative location of the bound ligand within the minor groove.

Strong Hydrogen Bond Is Formed between the NH Proton of the Amide Linker between the Indole and Benzofuran Subunits and a Thymine (T10) on the Modified Strand. The close association between the indole and the benzofuran subunits and the modified strand is primarily the result of a

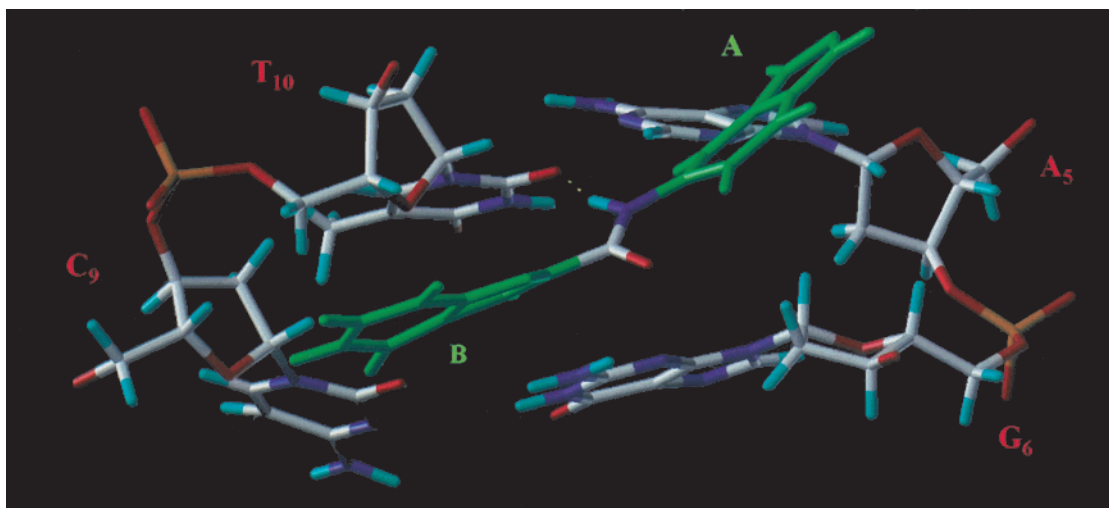


FIGURE 4: Section of the averaged structure for the top seven base pairs from the last 60ps of the rMD calculation for the adozelesin duplex adduct (300 K). Illustration shows the major hydrogen bond formed between the linking moiety and the carbonyl of thymine (T10).

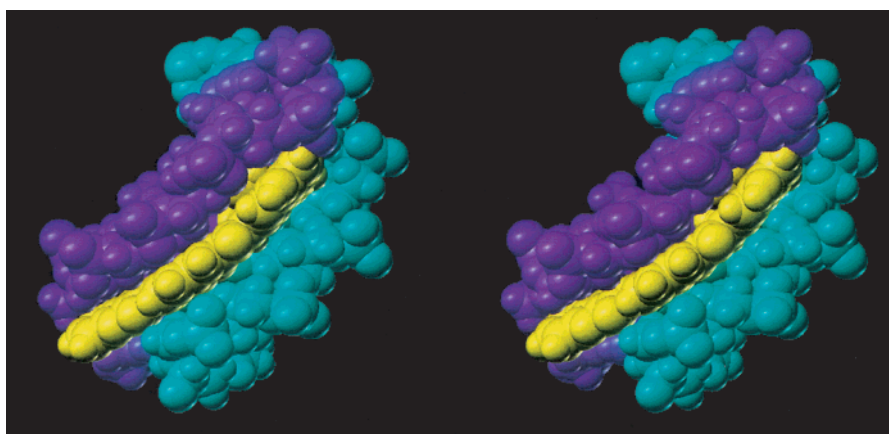


FIGURE 5: Stereo figures showing the averaged structure for the top seven base pairs from the last 60ps of the rMD calculation for the adozelesin duplex adduct (300 K). Adozelesin is shown in yellow the DNA duplex in cyan and blue (modified strand).

strong hydrogen bond between the NH of the amide linker moiety between the indole and benzofuran subunits and a carbonyl on thymine (T10, 2.11 Å). This hydrogen bond is fully occupied throughout all of the rMD calculations and effectively anchors the bound adozelesin to the modified DNA strand. Interestingly, unlike the much weaker hydrogen bond observed between the exocyclic NH₂ of guanine and the carbonyl of this linker, this hydrogen bond causes little or no detectable distortion in either the hydrogen bond base pair or the bound ligand.

Distortion around a Central Guanine (G6) Provides Additional Ligand/Duplex Hydrogen-Bonding Opportunities. The distortion of the central G•C (G6) base can clearly be seen within the ¹H NMR data. The relative intensities of the internucleotide and intranucleotide connectivities for the PuH8/PyH6 to H1' and PuH8/PyH6 to H2' and H2'' protons suggest that all 14 of the base pairs except guanine G6 are in the more commonly observed anti-conformation. From the relative NOE intensities of the signals from the sugar protons on guanine G6 into the base directly to the 3' and 5' side, it would appear that this deoxyribose sugar has adopted the normally less favored C3'-endo conformation. This would appear to be a similar result to that observed within the (+)-CC-1065 adduct formed with the duplex 5'-GGCGGAG-TTA*GG-3'/3'-CCGCCTC⁺AATCC-5' (A*-covalently modi-

fied adenine,⁺-C18), where it is proposed that C18 was present in a C3'-endo conformation (17).

Linking Moiety between the Adozelesin Subunits (B/C) Can Play an Important Role in Determining the Sequence Selectivity of Adozelesin and May Provide an Insight into the DNA Overwinding Observed in (+)-CC-1065 Adducts. Previous studies with bizelesin have indicated the important role that the central linker has in determining the sequence specificity for this dimeric compound. Within the cross-linked duplex adduct formed by bizelesin and 5'-TAATTA, the central base pairs were found to be in either an open or Hoogsteen conformations stabilized by the hydrogen bonding involving the ureylene linker. This NMR and molecular dynamics study indicates that a similar situation also exists within the monomeric CPI analogues, in that the linking functions between the subunits may have a significant effect on the binding of these ligands to double-stranded DNA. Previous molecular modeling studies have indicated that the (+)-CC-1065 and the CPI minor groove-binding ligands should have a strong sequence preference for sequences containing just A•T base pairs. These results have never been supported by DNA-footprinting experiments which have found the sequence preference is always restricted to 5'-TTA*-3', despite the ligand being positioned over at total of 5 base pairs (including the modified adenine) within the

minor groove.

Previous studies with (+)-CC-1065 have also shown that the ethano bridges of the B and C subunits in the natural product are responsible for the observed delayed lethality and DNA overwinding. Interestingly, in (+)-CC-1065, the NH of the amide linker is incorporated into a ring system incorporating these ethano bridges and hence the amine is unable to interact with the DNA as observed in this adozelesin duplex adduct. Studies are already underway in this laboratory to synthesize a closely related (+)-CC-1065 and adozelesin duplex-adduct using the same DNA sequence. It is with hope that results from this comparative study will finally establish the exact structural origins of the DNA overwinding in (+)-CC-1065 adducts. Obviously, the origins of the overwinding must originate from ligand-DNA interactions around the amide linker between the subunits. The observation of significant hydrogen bonding in this adozelesin duplex adduct would appear to indicate a significant difference in the binding mechanism for these two closely structurally related compounds and we suspect holds the key to the inability of adozelesin to overwind DNA and cause delayed lethality observed with (+)-CC-1065.

ACKNOWLEDGMENT

We thank Dr. George Gray at Varian, Palo Alto for his help accumulating the data on their Varian Innova 600 MHz NMR data and Dr. Michael D. Threadgill, University of Bath, for proof-reading this manuscript.

REFERENCES

- Hanka, L. J., Dietz, A., Gerpheide, S. A., Kuentzel, S. L., and Martin, D. G. (1978) *J. Antibiot.* **31**, 1211–1217.
- Martin, D. G., Biles, C., Gerpheide, S. A., Hanka, L. J., Krueger, W. C., McGovren, J. P., Miszak, S. A., Neil, G. L., Stewart, J. C., and Visser, J. (1981) *J. Antibiot.* **34**, 1119–1125.
- Lin, C. H., Beale, J. M., and Hurley, L. H. (1991) *Biochemistry* **30**, 3597–3602.
- McGovren, J. P., Clarke, G. L., Pratt, E. A., and Dekoning, T. F. (1984) *J. Antibiot.* **37**, 63–70.
- Neil, G. L., Clarke, G. L., and McGovren, J. P. (1981) *Proc. Am. Assoc. Cancer Res.* **22**, 1244.
- Fleming, G. F., Ratain, M. J., O'Brien, S. M., Vogelzang, N. J., and Earhart, R. H. (1992) *Proc. Am. Assoc. Cancer Res.* **33**, 265.
- Burris, H., Earhart, R., Kuhn, J., Shaffer, D., Smith, L., Weiss, G., Kasunic, D., Radbury, G., Campbell, L., and Von Hoff, D. D. (1992) *Proc. Am. Assoc. Cancer Res.* **33**, 520.
- Reynolds, V. L., Molineux, I. J., Keplan, D. J., Swenson, D. H., and Hurley, L. H. (1985) *Biochemistry* **24**, 6228–6237.
- Zakrewska, K., Randrianarivelo, M., and Pullman, B. (1987) *Nucleic Acids Res.* **15**, 5775–5785.
- Lin, C. H., and Hurley, L. H. (1990) *Biochemistry* **29**, 9503–9507.
- Lin, C. H., and Patel, D. (1995) *J. Mol. Biol.* **248**, 162–179.
- Hurley, L. H., Warpehoski, M. A., Lee, C.-S., McGovren, J. P., Scahill, T. A., Kelly, K. C., Wicnienski, N. A., Gebhard, I., and Bradford, V. S. (1990) *J. Am. Chem. Soc.* **112**, 4633–4649.
- Seaman, F. C., and Hurley, L. H. (1993) *Biochemistry* **32**, 12577–12585.
- Seaman, F. C., and Hurley, L. H. (1995) *Nat. Struct. Biol.*
- Thompson, A. S., and Hurley, L. H. (1995) *J. Mol. Biol.* **252**, 86–107.
- Thompson, A. S., Fan, J.-Y., Sun, D., Hansen, M., and Hurley, L. H. (1995) *Biochemistry* **34**, 11005–11016.
- Hurley, L. H., and Draves, P. H. (1993) In *Molecular Aspects of Anticancer Drug-DNA Interactions* (Neidle, S., and Waring, M. J., Eds.) Vol. I, pp 89–133, Macmillan Press Ltd., Basingstoke, England.
- Thompson, A. S., and Hurley, L. H. (1995) *J. Am. Chem. Soc.* **117**, 2371–2372.
- Gait, M. J., Ed. (1984) *Oligonucleotide Synthesis-A Practical Approach*, IRL Press, Oxford, England.
- Sklenar, V., and Bax, A. (1987) *J. Magn. Reson.* **74**, 469–479.
- Blake, P. R., and Summers, M. F. (1990) *J. Magn. Reson.* **86**, 622–624.
- Bax, A., Griffey, H., and Hawkins, B. (1983) *J. Magn. Reson.* **55**, 301–315.
- Purcel, W. P., and Singer, J. A. (1967) *J. Chem. Eng. Data* **12**, 235–246.
- Gasteiger, J., and Marsili, M. (1980) *Tetrahedron* **36**, 3219–3228.
- Young, M. A., Jayaram, B., and Beveridge, D. L. (1997) *J. Am. Chem. Soc.* **119**, 59–69.
- Blanco, M. (1991) *J. Comput. Chem.* **12** (2), 237–247.
- Hansen, M., and Hurley, L. H. (1995) *J. Am. Chem. Soc.* **117**, 2421–2429.
- Auffinger, P., Louise-May, S., and Westhof, E. (1995) *J. Am. Chem. Soc.* **117**, 6720–6726.
- Walker, G. S., Fagerness, P. E., Farley, K. A., and Miszak, S. A. (1997) *J. Heterocycl. Chem.* **34**, 295–299.
- Chary, K. V. R., Hosur, R. V., and Govil, G. (1987) *Biochemistry* **26**, 1315–1322.

BI9926532